

A Combined Central-Local Volt/Var Approach in Distribution Systems with High PV Uptake

Seyyed Mahdi Noor Rahim Abadi

*Engineering and Computer Science
The Australian National University
Canberra, Australia
mahdi.noori@anu.edu.au*

Paul Scott

*Engineering and Computer Science
The Australian National University
Canberra, Australia
paul.scott@anu.edu.au*

Sylvie Thiébaux

*Engineering and Computer Science
The Australian National University
Canberra, Australia
sylvie.thiebaux@anu.edu.au*

Abstract—Massive integration of residential photovoltaic (PV) generation has caused overvoltage issues in distribution systems. In this paper, we propose a two-stage central-local solution using the unused capacity of the residential inverters. Unlike similar approaches, we propose to benefit from a wider range of information available at the local level, i.e., both voltage magnitude and real power injection. To achieve this, in the first stage, a central controller periodically takes measurement throughout the network to determine a scalar function mapping two local variables, namely real power injection/demand and voltage magnitude, to the reactive power of each inverter. The second stage is a local feedback controller that determines the inverter reactive power injection/absorption, using the provided functions and local measurements. The effectiveness of the proposed design is assessed on a real 30-bus LV feeder. The results are compared with the Volt/Var control suggested by IEEE standard 1547 and an optimal solution with complete information. Our simulations show that our design obtains near-optimal results, and keeps the voltages within the predefined limit in more scenarios than the IEEE standard 1547 while decreasing the required reactive power by 60%, and the real power loss by 3.3%.

Index Terms—Renewable integration, distribution system, Volt/Var, optimal power flow, real-time control

I. INTRODUCTION

In the last decade, the growing adoption of photovoltaic (PV) panels has led to new challenges in operating distribution systems [1]. Maximum PV generation typically happens simultaneously with low residential load consumption. This in turn may cause reverse power flow in the grids with high PV penetration, which can potentially cause overvoltage, especially in weak grids. Traditional distribution voltage control methods, i.e. using capacitor banks, on-load tap changers and step voltage regulators, were designed to control voltage fluctuations due to slow changes in demand. These methods are not adequate to respond to fast and random variations of PV system outputs, and are potentially expensive to install throughout the distribution system [2]. Utilization of reactive power support capability of smart inverters is an effective alternative, as they can provide fast and dynamic response which can reduce investment costs [3].

Different control strategies exist to get the preferred behaviour out of installed inverters in the distribution systems.

A closed-loop control strategy can be an effective way of regulating the point of common coupling (PCC) voltage of a PV system that employs the full potential of smart inverters. In closed-loop Volt/Var controllers, real-time measurements are compared with a reference value. Based on their mismatch, the controllers will adjust the reactive output powers to follow the reference value [4]. Various techniques exist in the literature for the implementation of closed-loop Volt/Var control strategies, which can be broadly classified based on the communication requirements as centralized, decentralized and local.

In centralized approaches, a central entity periodically collects measurements throughout the network, and will typically determine the reference values by solving some sort of optimal power flow (OPF) problem at regular time intervals [5]. Although these methods can successfully coordinate all the voltage regulation devices and achieve an optimal solution, it can be impractical to solve an OPF for fast-changing PV generators in large distribution systems. Decentralized methods can decompose an overall optimization problem into small sub-problems and solve them in parallel [6]. This can speed up solve times, but will still struggle to cope with fast-changing PV generators. Local controllers can provide fast responses to network operation changes. However, due to limited information available in these approaches, they lack a system-wide coordination and optimization. This can lead to unnecessary reactive power injection/absorption in some scenarios, which in turn increases line losses in the entire system or the opposite in some scenarios, i.e., under-utilization of available resources, which may lead to failure to keep the voltages within the network limits.

Combined local and central approaches benefit from both system-wide coordination of central approaches and fast response of local approaches. In [7], the authors use a centralized optimization to tune the local controller parameters based on the forecasted data over a day. In [8], a two-level control architecture is proposed, wherein the lower level, a piecewise linear Volt/Var function is implemented, which reacts promptly to voltage variations. In the higher level, a central controller periodically solves an OPF, and sends adjustments to the lower level, to modify controller parameters. In [9] and [10], affine functions at the central level are obtained, relating

the reactive power of each inverter to local changes in real power injection. Then, in real-time at the local level using the assigned functions and local measurement, the inverter reactive powers are calculated. In all the aforementioned literature, at the local level, the reactive power of inverters are obtained either based on deviations in voltage magnitude or real power injections, but not both together. As mentioned above, the main shortcoming of the local controller approaches is that they have access to limited information. Neglecting one of the sources of information (voltage magnitude or real power injection) misses an opportunity to better optimise the system. Therefore, in this paper, we propose an approach to benefit from both sources of information available at the local level.

We propose a two-stage Volt/Var scheme. In the first stage, a central controller periodically makes measurement throughout the network. Considering an uncertainty interval in the uncertain parameters (PV generation and residential demand), two scenarios are developed, one for the best case and one for the worst case. Then, three optimal power flows are solved, one for each scenario (measurement, the worst case, and the best case), to obtain the optimal reactive power injection/absorption of each inverter. Next, through a set of steps, detailed in section III, a piece-wise linear Volt/Var function is obtained for each inverter in each scenario. Then, by applying linear interpolation between Volt/Var functions of each inverter, a scalar function of two variables, namely real power and voltage magnitude, is constructed and assigned to each inverter. In this way, both the locally available information will be used in the second stage. The second stage is a local feedback control that based on the calculated function in the first stage, and local real power injection and voltage magnitude measurement determine the reactive power contribution. To investigate the effectiveness of the proposed approach, we simulate it on a 30-bus distribution system and find it achieves near-optimal performance.

The rest of this paper is organized as follows. In section II, the problem formulation is presented. In section III, we introduce our proposed method. Simulation results are reported in section IV. Finally, section V concludes this paper.

II. PROBLEM FORMULATION

Fig. 1 shows a simple two-bus system where extra real PV power is injected to the grid. This injected power may produce a voltage rise at the PCC which can be approximated by:

$$V_i - V_k = \frac{r_{ik}P_i^{inj} + x_{ik}Q_i^{inj}}{V_i} \quad (1)$$

where V_i is the voltage magnitude at the connection point, r_{ik} and x_{ik} are resistance and reactance of the line between buses i and k , P_i^{inj} and Q_i^{inj} are the injected real and reactive powers from the connection point at bus i to the grid, respectively. The voltage rise problem can be managed by proper control of reactive powers through remaining unused capacity of the inverters. Notice that the arrow directions in Fig. 1 denote the assumed sign for the variables, rather than enforcing a one-way flow of power.

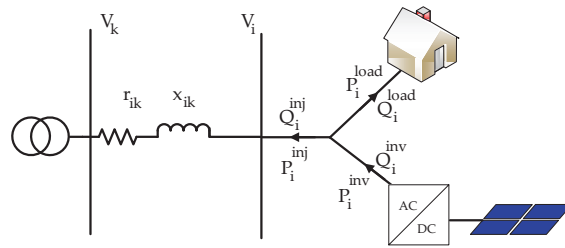


Fig. 1. A simple two bus feeder showing the reverse power flow.

III. PROPOSED METHOD

In this section, we describe our proposed two-stage Volt/Var control. In the first stage based on the following steps we calculate the reactive power of each inverter as a scalar function of local real power injection and voltage magnitude. Before getting to the details of each step, here is an overview of the process.

In the first stage, we begin by collecting measurements throughout the network. We assume that the PV generation and the residential demand between two measurements belong to the following uncertainty sets:

$$P^{inv} \in [P_0^{inv} - \Delta P^{inv}, P_0^{inv} + \Delta P^{inv}] \quad (2a)$$

$$P^{load} \in [P_0^{load} - \Delta P^{load}, P_0^{load} + \Delta P^{load}] \quad (2b)$$

where P_0^{inv} and P_0^{load} are the PV and demand at the measurement point, respectively. ΔP^{inv} and ΔP^{load} indicate the possible deviations from the measurement between two consecutive measurement point. Based on the uncertainty interval (2), we develop two scenarios. In the first scenario we consider the worst case from feeder voltage perspective, for example in a generation dominated moment the worst case happens when all the PVs reach to their maximum and all the demands decrease to their minimum value in the uncertainty interval. In second scenario we consider the opposite (the best case), i.e., all the demands reach to their maximum and all the PVs decrease to their minimum value in the uncertainty interval. Then, an OPF is solved for each of these scenarios to obtain the minimum reactive power required from each inverter to keep the voltages within the limit (*Step 1*). Next we want to calculate a piece-wise linear Volt/Var function for each inverter. The slope of the function shows how much a change in reactive power injection of a bus, would change its voltage magnitude. An accurate way to obtain the slope, is to use the inverse Jacobian matrix for each operating point (*Step 2*). Considering the optimal point obtained from *Step 1* and the slope obtained in *Step 2* we can determine a line (*Step 3*). By enforcing the inverter limitations and considering a symmetrical design for the piece-wise linear function, we obtain the droop curve (*Step 4 and 5*, shown in Fig. 2). By repeating *Step 1* to *Step 5* for the other two scenarios, we obtain a piece-wise linear curve for each of them (*Step 6*). The last step is to combine the piece-wise linear functions together,

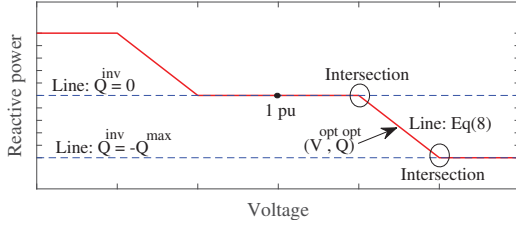


Fig. 2. Droop curve designed for an operating point where $Q_i^{opt} \leq 0$.

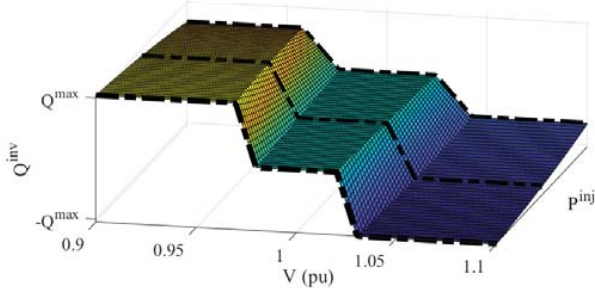


Fig. 3. A sample of the proposed scalar function of the two variables, real power injection, and voltage magnitude, for the local controllers. The three black-dotted lines show the piece-wise linear curves obtained from the three scenarios.

through linear interpolation, which makes the reactive power of each inverter a scalar function of local real power injection (through interpolation) and voltage magnitude (the piece-wise linear function), shown in Fig. 3. In what follows, we describe each step in detail.

Step 1: The first step is to formulate an OPF to obtain the minimum reactive power support, required from the inverters to keep all the voltages within the accepted limit. We use the *Distflow* model to represent the power flow equations, as the *Distflow* formulation is well-suited for radial distribution systems with a tree structure, as shown in [11]. In the *Distflow* formulation, a power network is represented by a connected graph $\mathcal{G} = (\mathcal{N}, \mathcal{B})$, where each node represents a bus and each link represents a line or branch. $\mathcal{N} = \{1, \dots, n\}$ denotes set of buses with cardinality $|\mathcal{N}| = n$ and $\mathcal{B} \subseteq \mathcal{N} \times \mathcal{N}$ denotes the set of all branches and (i, k) or $i \rightarrow k$ shows a branch from bus i to bus k . For every bus $i \in \mathcal{N}$, let v_i denote the squared voltage magnitude. Also, let $P_i^{inj} = P_i^{inv} - P_i^{load}$ denote the real power injected to the grid from bus i , and $Q_i^{inj} = Q_i^{inv} - Q_i^{load}$ denote the reactive power injected to the grid from bus i . For every branch $(i, k) \in \mathcal{B}$, let $z_{ik} = r_{ik} + jx_{ik}$ denote the complex impedance of the line, and $l_{ik}(t)$ denote the squared current magnitude from bus i to bus k . Also, let $S_{i,k} = P_{ik} + jQ_{ik}$ be the sending-end complex power from bus i to bus k . It is also assumed that the substation voltage v_1 is given. What follows is the OPF formulation:

$$\min \sum_{i=1}^n Q_i^{aux} \quad (3a)$$

$$P_j^{inj} = \sum_{k:j \rightarrow k} P_{jk} - (P_{ij} - r_{ij}l_{ij}) \quad \forall j \in \mathcal{N} \quad (3b)$$

$$Q_j^{inj} = \sum_{k:j \rightarrow k} Q_{jk} - (Q_{ij} - x_{ij}l_{ij}) \quad \forall j \in \mathcal{N} \quad (3c)$$

$$v_j = v_i - 2(r_{ij}P_{ij} + x_{ij}Q_{ij}) + (r_{ij}^2 + x_{ij}^2)l_{ij} \quad \forall (i, j) \in \mathcal{B} \quad (3d)$$

$$l_{ij} = \frac{P_{ij}^2 + Q_{ij}^2}{v_i} \quad \forall (i, j) \in \mathcal{B} \quad (3e)$$

$$P_i^{inv^2} + Q_i^{inv^2} \leq S_i^{max^2} \quad \forall i \in \mathcal{N} \quad (3f)$$

$$Q_i^{aux} \geq -Q_i^{inv}, \quad Q_i^{aux} \geq Q_i^{inv} \quad \forall i \in \mathcal{N} \quad (3g)$$

where (3b)-(3e) denote the *Distflow* model, and (3f) denotes the apparent power equation, enforcing the inverter capacity constraint. Q_i^{aux} is a positive auxiliary variable defined to linearize the absolute value of Q_i^{inv} through constraints (3g).

Remark: Problem (3) is not convex due to the quadratic equality constraint (3e). As shown in [12], the SOCP relaxation of the *Distflow* model suggested by [11] is not exact when the ampacity constraints of the lines are binding, i.e., the answer provided by the OPF will not lie within the feasible region. Also, as shown in [13], although the linear *Distflow* model is convex, it overestimates the voltage magnitude, and in turn, significantly increases the reactive power required to keep the voltages within the limit. Our simulations in a moderately sized distribution system show that if the variables are properly bounded, problem (3) can be efficiently solved by solvers such as *IPOPT*, and the answer obtained through solving the non-convex model is feasible and superior to the answer obtained by the linear *Distflow* model. For an extremely large system, one can replace the non-convex power flow model with the linear *distflow model* model, and use the rest of our approach.

Step 2: Calculate the inverse Jacobian matrix. The Jacobian matrix of the power flow equations can be formulated as follows:

$$\mathbf{J} = \begin{bmatrix} \frac{\partial \mathbf{P}^{inj}}{\partial \boldsymbol{\delta}} & \frac{\partial \mathbf{P}^{inj}}{\partial \mathbf{V}} \\ \frac{\partial \mathbf{Q}^{inj}}{\partial \boldsymbol{\delta}} & \frac{\partial \mathbf{Q}^{inj}}{\partial \mathbf{V}} \end{bmatrix} \quad (4)$$

where \mathbf{J} is the Jacobian matrix, operator ∂ denotes partial derivative, and $\boldsymbol{\delta}$ is the vector of voltage angles. Defining $Y_{ii} \equiv G_{ii} + jB_{ii}$, and using the bus injection model [14], we obtain:

$$P_i^{inj} = G_{ii}V_i^2 + \sum_{\substack{k=2 \\ k \neq i}}^n V_i V_k |Y_{ik}| \cos(\theta_{ik} + \delta_k - \delta_i) \quad (5a)$$

$$Q_i^{inj} = -B_{ii}V_i^2 - \sum_{\substack{k=2 \\ k \neq i}}^n V_i V_k |Y_{ik}| \sin(\theta_{ik} + \delta_k - \delta_i) \quad (5b)$$

where $Y_{ik} = |Y_{ik}| \angle \theta_{ik}$ shows the admittance between buses i and k , and δ_i denotes the voltage angle at bus i . Taking the partial derivative from (5), we obtain the Jacobian matrix. Based on the inverse Jacobian matrix, we obtain the following:

$$\Delta V_k = \sum_{i=2}^n \left(\frac{\partial V_k}{\partial P_i^{inj}} \Delta P_i^{inj} + \frac{\partial V_k}{\partial Q_i^{inj}} \Delta Q_i^{inj} \right) \quad (6)$$

Considering $Q_i^{inj} = Q_i^{inv} - Q_i^{load}$, we obtain the voltage sensitivity of bus k to changes in its inverter reactive power as follows:

$$\Delta V_k = \frac{\partial V_k}{\partial Q_k^{inv}} \Delta Q_k^{inv} \quad (7)$$

Step 3: Consider the sensitivity of voltage magnitude to reactive power at each bus as slope of a line. Considering the slope, and the pair (V_k^{opt}, Q_k^{opt}) obtained from *Step 1*, we obtain the following line equation:

$$Q_i^{inv} - Q_i^{opt} = \frac{-1}{\frac{\partial V_i}{\partial Q_i^{inv}}} (V_i - V_i^{opt}) \quad (8)$$

Notice that the term $\frac{\partial V_i}{\partial Q_i^{inv}}$ is always positive if the system is in normal operating condition. This is because, by definition, if V-Q sensitivity is positive for every bus, the system is voltage stable, and if V-Q sensitivity is negative for at least one bus, the system is voltage unstable [15]. Therefore, the negative sign in (8) ensures a negative slope for Q-V droop curves for normal operating conditions.

Step 4: Intersect line (8) with two lines $Q_i^{inv} = 0$ and $Q_i^{inv} = -Q_i^{max}$, when $Q_i^{opt} \leq 0$ (see horizontal lines in Fig. 2), and similarly with two lines $Q_i^{inv} = 0$ and $Q_i^{inv} = Q_i^{max}$, when $Q_i^{opt} \geq 0$. The intersection will give two voltage and reactive power pairs.

Step 5: Assuming a symmetrical design for the piecewise linear curve over the $1pu$ voltage, we obtain the droop function. Fig. 2 shows such a design for a scenario where $Q_i^{opt} \leq 0$. Also, in this step, we enforce a new rule to increase the efficiency of the design. Having a large dead-band can prevent unnecessary reactive power usage. Therefore, we consider a minimum symmetrical dead-band for the droop, equal to the dead-band of IEEE 1547 standard. We left a more systematic design of the dead-band to future works.

Step 6: Repeat *Step 1* to *Step 5* for the two other scenarios, i.e., the best and worst cases. By doing so, we obtain three droop curves for the three different operating points.

Step 7: Perform a linear interpolation between the three curves obtained in *Step 6*. This will result in a scalar function of two variables, namely real power injection and voltage magnitude for each inverter. Fig. 3 shows an example of such a design. Notice that as P_i^{inv} increases, the available reactive power decreases due to the inverter capacity limitation.

In the second stage, each local controller measures the local voltage and real power injections to the grid in real-time. Then, using the function from stage one, it determines the value of reactive power support. This process can be repeated periodically (e.g., every 5 minutes) to improve the performance. In the second stage we consider a safety rule. We consider that if in real time the real power injection changes significantly from the measurement (more than twice the uncertainty bound) the fixed droop, suggested by IEEE 1547, replaces the function.

IV. SIMULATIONS AND RESULTS

We consider a real 30-bus modern underground LV feeder with $R/X \approx 2$ located in Hobart, Australia shown in Fig. 4.

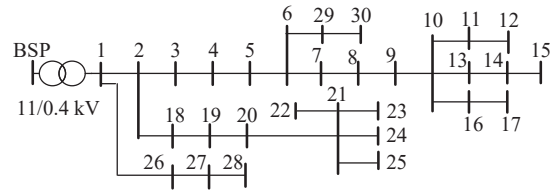


Fig. 4. 30-bus low-voltage feeder.

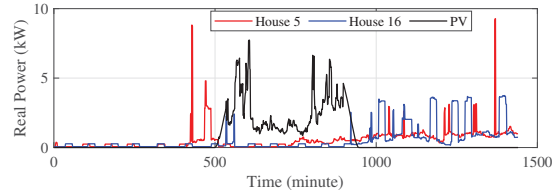


Fig. 5. Load and PV minutely patterns. Load pattern at bus 5 and 16 are presented here to show different patterns are used in each bus.

One minute resolution load and PV data is obtained based on the CREST demand model [16], shown in Fig. 5. Each of the 29 different residential customers (*Bus 1* is considered as the slack bus) have a different load pattern, and 50% have rooftop PV with a correlated solar input. To test the performance of the proposed method, we conduct two tests. In the first one, we consider uniform changes in real power injection and compare the performance of our design with the fixed droop curve, and also with the optimal answer of solving the OPF (3). In the second test, we use the CREST demand model. The resolution of the data is one minute, and we collect measurements every 5 minutes. The metrics of interest are, voltage profile, total reactive power support, and real power loss in the network conductors. The PV inverters are sized at 9kVA.

A. Uniform Change in Data

The linear interpolation used in *Step 7* can closely follow the optimal answer so long as the network operating point does not change significantly. For example, Fig. 6 shows the reactive power support of all the inverters for the three schemes for minute 604, where the PV generation is at its maximum. ΔP^{inv} and ΔP^{load} are considered 5% of the measurement value, and we uniformly increase the PV and decrease the demand from 0% to 7%. It can be seen that for 0% and 5% the results are exactly equal to the optimal answer, and for the other scenarios are near optimal. This result was expected, since we solved an OPF for the measurement and the worst case i.e., 5% uniform increase in PV and 5% uniform decrease in demand of all the buses.

The mentioned scenarios are for the cases where the system is operated near its voltage limit. Fig. 7 shows the reactive power support for minute 834, where all the voltages without any reactive power support are in the acceptable limit. This case is of utmost importance as a considerable portion of a day is made up of times where no reactive support is necessary.

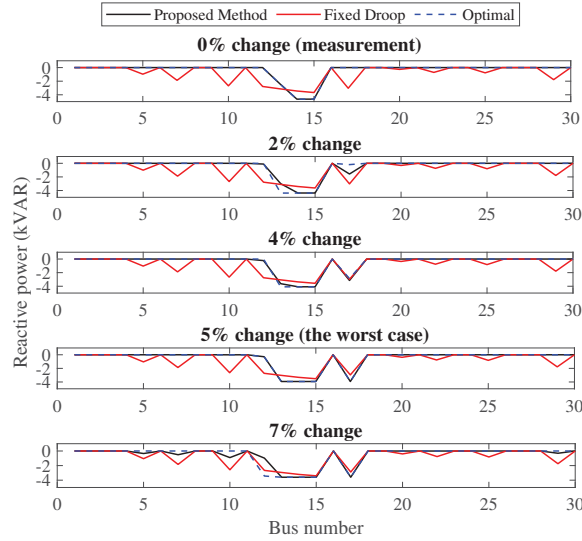


Fig. 6. Injected reactive power at each bus in minute 604, for each method and varying uniform % changes from the stage 1 forecast power. Since we solve an OPF for the measured operating point and the worst case (5% deviation in PV and demand) the results for these scenarios happen to be exactly equal to the optimal solution.

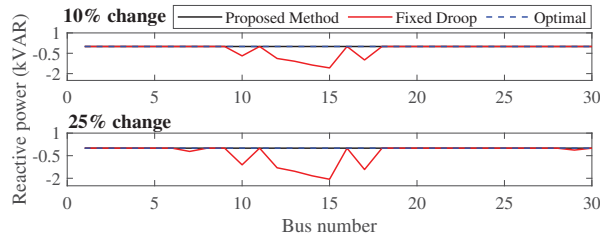


Fig. 7. Reactive power support for different levels of uniform change from measurement in minute 834.

Using a fixed droop will significantly increase real power loss in the conductors for long hours in a day, which can be prevented with our method. For example, our approach can decrease the real power loss by 5% compared to the fixed droop in minute 834, when the operating point is subjected to 25% uniform variation relative to the stage one forecast.

B. Real Data: Detailed for Some Minutes

In this part, we test the performance of our design using the data from the CREST demand model. For the minutes that the bus voltages are well-below the limit, the proposed method avoids wastefully using reactive power like the optimal solution. For example, Fig. 8 shows the performance of the three schemes when measurements are gathered in minute 835, and used for the next 5 minutes (Only three minutes are reported here to prevent repetition).

In the minutes where the bus voltages are close to their limit, requiring reactive support from more than one inverter, is more challenging, especially when changes in demand and generation are out of the designed uncertainty bound. Fig. 9

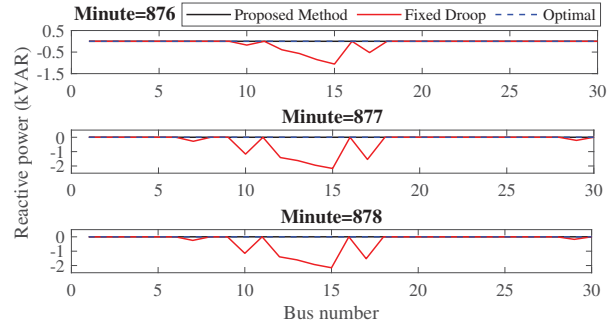


Fig. 8. Reactive power support at minutes 876 to 878 when the measurement is collected at minute 834.

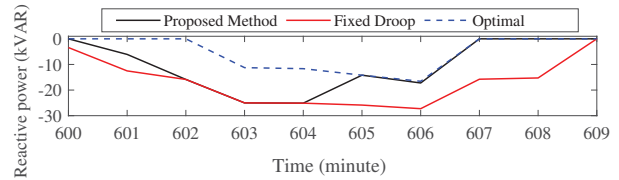


Fig. 9. Aggregated reactive power support of the three schemes for minutes 600 to 609, with measurements at minutes 600 and 605.

shows the aggregated reactive power support for the three different schemes in minutes 600 to 609. The measurements are collected in minutes 600 and 605 and used for their corresponding next 5 minutes. The aggregated reactive power injections in the proposed design is less than or equal to the fixed droop in all of the minutes and buses. Also, in minutes 603 to 605, the injection powers of most buses change significantly from the measurement in minute 600, more than 140% in most of the buses. This would activate the safety feature described in section III. As a result, in these minutes, the inverters are using the standard droop, and consequently, the proposed and fixed droop obtain the same results.

C. Real Data: Over the whole day

In this subsection, we look at the three schemes over a whole day. The simulation results are summarized in Fig. 10, and detailed in Table I. We can see that the proposed method successfully keeps the voltages within the accepted range over the whole day, while managing to use less reactive power than the fixed droop, and it achieves near-optimal real power loss. It decreases the required reactive power by 61%, and the real power loss by 3.3% compared to the fixed droop approach.

D. Further Improvement on the Proposed Design

Our proposed method is based on linear interpolation between the three operating points (the measurement, the worst case, and the best case). Therefore, as the uncertainty interval (ΔP^{inv} and ΔP^{load}) expands, the performance of our method deteriorates, which is confirmed by our simulations. To tackle this problem, we propose a further improvement in the design by partitioning the uncertainty interval into multiple smaller sections, and then repeat the same process as discussed in

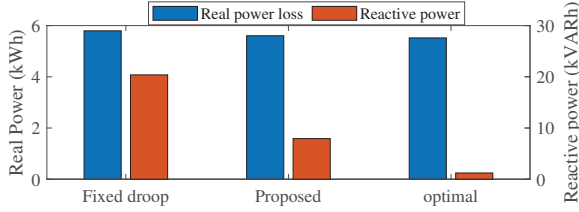


Fig. 10. Aggregate reactive power support and real power loss of the three schemes over the whole day.

TABLE I

AGGREGATED REACTIVE POWER SUPPORT AND REAL POWER LOSS USING DIFFERENT SCHEMES.

Approach	Aggregated reactive power (kVARh)	real power loss (kWh)	No. of voltage violation
Fixed droop	20.374	5.795	0
Proposed	7.924	5.603	0
Optimal	1.217	5.537	0
No Control	0	5.519	11

TABLE II

AGGREGATED REACTIVE POWER SUPPORT AND REAL POWER LOSS USING THE IMPROVED METHOD.

Approach	Aggregated reactive power (kVARh)	real power loss (kWh)	No. of voltage violation
Proposed $\gamma = 2$	7.924	5.603	0
Proposed $\gamma = 4$	7.548	5.591	0
Proposed $\gamma = 6$	7.126	5.579	0
Proposed $\gamma = 8$	7.074	5.575	0

section III. To illustrate, consider an uncertain parameter $x \in [x_0 - \Delta x, x_0 + \Delta x]$, where x_0 denotes the value of x at the measurement time. The proposed partitioning is as follows:

$$\gamma = 2 : [x_0 - \Delta x, x_0, x_0 + \Delta x] \quad (9)$$

$$\gamma = 4 : [x_0 - \Delta x, x_0 - \frac{\Delta x}{2}, x_0, x_0 + \frac{\Delta x}{2}, x_0 + \Delta x]$$

$$\vdots$$

where γ is an arbitrary even number which denotes the number of segments to cut the uncertainty interval. Notice that $\gamma = 2$ is the same as having three operating points, the measurement, the worst case, and the best case. As the γ increases, we have access to more scenarios. The idea is to solve OPF (3) for each of the operating points to obtain additional Volt/Var curves and perform linear interpolation between them all. Table II summarizes the results using the improved method over the whole day. It can be seen that the performance of our approach improves as the number of partitions increases.

V. CONCLUSION

In this paper, a two-stage real-time Volt/Var control approach is proposed to maximize the opportunity for an inverter to provide reactive power support. In the first stage, we periodically gather network-wide information, and systematically update local control parameters to ensure near-optimal

operation of smart inverters. In the second stage, a real-time feedback control is designed that decides about the reactive power contribution of its inverter based on the local voltage and real power injection. Our simulations show that our design obtains near-optimal results, that can keep the voltages in more scenarios than the IEEE standard 1547 within the predefined range, while decreasing the required reactive power by 60%, and the real power loss by 3.3%. We also provide further improvement on our design, by a novel partitioning in the uncertainty interval, that can further decrease the reactive power and real power loss, at the cost of more computation at each interval. A further extension in our work is to consider real power curtailment, as in some scenarios, there would be no solution to the overvoltage problem, using only reactive power of inverters.

REFERENCES

- [1] S. Hashemi and J. Østergaard. Efficient control of energy storage for increasing the PV hosting capacity of LV grids. *IEEE Transactions on Smart Grid*, 9(3):2295–2303, 2018.
- [2] M. Zeraati, M. E. Hamedani Golshan, and J. M. Guerrero. Distributed control of battery energy storage systems for voltage regulation in distribution networks with high PV penetration. *IEEE Transactions on Smart Grid*, 9(4):3582–3593, 2018.
- [3] S. M. N. R. Abadi, M. Mahmoodi, P. Scott, L. Blackhall, and S. Thiebaux. Active management of LV residential networks under high PV penetration. In *2019 IEEE Milan PowerTech*, pages 1–6, 2019.
- [4] B. K. Perera, P. Ciufo, and S. Perera. Point of common coupling (PCC) voltage control of a grid-connected solar photovoltaic (PV) system. In *IECON 2013 - 39th Annual Conference of the IEEE Industrial Electronics Society*, pages 7475–7480, 2013.
- [5] F. Olivier, P. Aristidou, D. Ernst, and T. Van Cutsem. Active management of low-voltage networks for mitigating overvoltages due to photovoltaic units. *IEEE Transactions on Smart Grid*, 7(2):926–936, 2016.
- [6] L. Wang, R. Yan, and T. K. Saha. Voltage management for large scale PV integration into weak distribution systems. *IEEE Transactions on Smart Grid*, 9(5):4128–4139, 2018.
- [7] Y. Chistyakov, E. Kholodova, K. Netreba, A. Szabo, and M. Metzger. Combined central and local control of reactive power in electrical grids with distributed generation. In *2012 IEEE International Energy Conference and Exhibition (ENERGYCON)*, pages 325–330, 2012.
- [8] H. S. Bidgoli and T. Van Cutsem. Combined local and centralized voltage control in active distribution networks. *IEEE Transactions on Power Systems*, 33(2):1374–1384, 2018.
- [9] R. A. Jabr. Linear decision rules for control of reactive power by distributed photovoltaic generators. *IEEE Transactions on Power Systems*, 33(2):2165–2174, 2018.
- [10] R. A. Jabr. Robust volt/var control with photovoltaics. *IEEE Transactions on Power Systems*, 34(3):2401–2408, 2019.
- [11] M. Farivar and S. H. Low. Branch flow model: Relaxations and convexification—part i. *IEEE Transactions on Power Systems*, 28(3):2554–2564, 2013.
- [12] M. Nick, R. Cherkaoui, J. L. Boudec, and M. Paolone. An exact convex formulation of the optimal power flow in radial distribution networks including transverse components. *IEEE Transactions on Automatic Control*, 63(3):682–697, 2018.
- [13] M. S. S. Abad, J. Ma, D. Zhang, A. S. Ahmadyar, and H. Marzoughi. Probabilistic assessment of hosting capacity in radial distribution systems. *IEEE Transactions on Sustainable Energy*, 9(4):1935–1947, 2018.
- [14] J. J. Grainger and W. D. Stevenson. *Power system analysis*. McGraw-Hill, 1994.
- [15] P. Kundur, Prabha, N. J. Balu, and M. J. Lauby. *Power system stability and control*, volume 7. McGraw-hill New York, 1994.
- [16] E. McKenna and M. Thomson. High-resolution stochastic integrated thermal–electrical domestic demand model. *Applied Energy*, 165:445–461, 2016.